https://doi.org/10.5194/egusphere-2024-957
Preprint. Discussion started: 15 April 2024

Evaluating the disaster risk levels associated with "Dragon Boat Water" in Guangdong China

Yamin Hu[1], Xiaocen Jiang[2], Juanhuai Wang[1], Liang Zhao[3], Guanrong Huang[4]

[1]Guangdong Climate Center, Guangzhou 510640, China
[2]Dongguan Meteorological Bureau, Dongguan 523082, China
[3]State Key Laboratory of Numerical Modeling for Atmosphere Sciences and Geophysical Fluid Dynamics (LASG), Institute of Atmospheric Physics, Chinese Academy of Sciences, Beijing 100029, China
[4]Shaoguan Meteorological Bureau, Shaoguan 512028, China

Correspondence to: Xiaocen Jiang (xiaocenj@126.com); Liang Zhao (zhaol@lasg.iap.ac.cn)

Abstract. Dragon Boat Water (DBW) is a period characterized by abundant precipitation and concentrated precipitation process in Guangdong province, China. The period often leads to severe flood disasters, resulting in substantial losses to both livelihoods and production. However, a comprehensive assessment of disaster risk during DBW has been lacking.

In this study, we utilized daily precipitation data spanning the years from 1995 to 2020, coupled with related disaster data from Guangdong. The Precipitation Comprehensive Intensity Index (*PCII*) and the DBW Comprehensive Disaster Index (*CDI*) were established. *PCII* and *CDI* were categorized into three levels using the percentile method. Moreover, we delved into the intricate relationship between these two indexes.

The results revealed that *PCII* falls into the three levels: extreme heavy, heavy, and normal, representing 19.2%, 30.8%, and 50%, respectively, with the peak occurring in 2008. Meanwhile, *CDI* comprises three levels: high, medium and low, accounting for 19.2%, 30.8% and 50.0%, respectively, with peak years closely aligning with those of *PCII*. Our calculations demonstrated a positive correlation between *PCII* and *CDI*, as well as between *PCII* and the occurrence of five types of disasters. Notably, heavier *PCII* levels had a more pronounce impact on crop damage, affected population numbers, and the direct economic loss, with the most substantial influence observed on the affected population. Though disaster data for 2022 has yet to be fully collated, based on *PCII* and *CDI*, we determined that 2022 experienced the fourth-highest precipitation and fifth-highest disaster level since 1995. This assessment concurs with the actual conditions observe in 2022. As a result, we propose that in the future, *PCII* and *CDI* can be invaluable tools for pre-disaster risk assessment, ongoing disaster monitoring, and expedited post-disaster evaluation.

1 Introduction

Guangdong Province, a monsoon-prone region situated in South China, is notable for experiencing some of the heaviest precipitation and the longest flood season in China (Ding and Chan, 2005; Luo et al., 2016; Zheng et al., 2016). The rainstorms

https://doi.org/10.5194/egusphere-2024-957
Preprint. Discussion started: 15 April 2024

and floods in Guangdong are predominantly concentrated during the period from April to September (Cheng et al., 2023). In particular, from late-May to mid-June, Guangdong often experiences heavy precipitation for several consecutive days, leading to severe flood disasters and significant disruptions to both social production and people's lives. (Lin et al., 2009; Luo et al., 2020; Liu et al., 2023). This concentrated period of precipitation, which coincides with the Dragon Boat Festival on the fifth day of the fifth lunar month, is known as "Dragon Boat Water" (DBW) (Lin et al., 2009).

According to a UNDRR (United Nations Office for Disaster Risk Reduction) report, over the past two decades, floods and storms have emerged as the most prevalent of global extreme weather events (Source: Centre for Research on the Epidemiology of Disasters United Nations Office for Disaster Risk Reduction, "The human cost of disasters: an overview of the last 20 years (2000-2019)", https://www.undrr.org/publication/human-cost-disasters-overview-last-20-years-2000-2019). In recent years, Guangdong also experienced some extreme precipitation and severe flood disasters during DBW (Lin et al., 2009; Wu et al., 2013; Sheng et al., 2023). For example, during the DBW period in 2022 (May 21-June 21), Guangdong experienced an average precipitation of 524.5 mm, representing a 54% increase from the previous year (334.6 mm), ranking as the third-highest in historical records. According to Natural Disaster Management System of the Ministry of Emergency Management, as of June 23 2022, a total of 1.2134 million people in Guangdong were affected by the disaster, with 12 fatalities attributed to it. The disaster also impacted 629.1 thousand hectares of crop and resulted in direct economic losses amounting to 4.958 billion CNY. To enhance understanding of the weather mechanism of DBW, current researches primarily focus on analysing the causes and statistical characteristics of typical and abnormal precipitation events during this period (Lin et al., 2009; Hu et al., 2013; Hu et al., 2016; Qian et al., 2020; Cheng et al., 2023; Sheng et al., 2023; Xie et al., 2023). To effectively prevent rainstorm and flood disasters, dynamic risk assessment is essential. However, there has been limited research on assessing the disaster risk associated with DBW precipitation (Huang et al., 2015).

As to rainstorm and flood disasters risk assessment, currently, researchers have primarily focused on three key areas. Firstly, GIS technology and hydrological dynamical models are utilized to construct flood disaster assessment models (Quan, 2014; Wu et al., 2015; Wu et al., 2019; Wang et al., 2022; Bouttier et al., 2024). The models consider factors related to flood risk, exposure and vulnerability of entities susceptible to disasters, and disaster prevention and mitigation capabilities. This approach aims to delineate disaster risk areas and create rainstorm flood risk maps. Secondly, researcher have employed hydrological dynamics and storm waterlogging simulation models to capture the dynamics of storm flooding, studying critical precipitation thresholds for disaster and water depth classifications (Xie et al., 2004; Peng et al., 2018; Song et al., 2018). Lastly, based on the disaster records and statistical methods, evaluation models have been constructed to assess rainstorm and flood disasters quantitatively. These models consider the relationship between rainstorms and disasters (Han et al., 2014).

In accordance with the chronological order of application scenarios, the risk assessment of rainstorm and flood disasters can be categorized into pre-disaster assessment, disaster tracking monitoring assessment, and post-disaster actual measurement assessment (Zhou et al., 2019). Currently, there are two types of pre-disaster assessments for the risk of rainstorms and flood disasters. One approach involves qualitative or quantitative predictions of the intensity, distribution, and potential losses from regional floods. This serves as the foundation for devising social development plans and disaster reduction strategies. The

https://doi.org/10.5194/egusphere-2024-957
Preprint. Discussion started: 15 April 2024

second approach focuses on conducting pre-disaster risk warnings based on prediction information related to disaster-causing factors, such as precipitation intensity, region, time, and critical precipitation, or utilizing constructed disaster assessment models (Hu H. et al., 2013; Zhou et al., 2019).

Most of the studies mentioned above rely on nowcasting for short-term weather forecasts to predict the risk of rainstorms and flood processes. Few studies have concentrated on forecasting disaster risk levels for the following month or season based on precipitation predictions made one month or one quarter in advance.

To address the needs of disaster prevention and mitigation, this study utilizes daily precipitation data and rainstorm and flood disaster data in Guangdong spanning from 1995 to 2020. A precipitation comprehensive intensity index and comprehensive disaster intensity of DBW are calculated and combined to perform a risk assessment. The goal is to conduct pre-disaster assessments, mid-disaster follow-up assessments, and post-disaster rapid assessments for DBW. This initiative aims to offer scientific guidance to emergency disaster reduction agencies and enhance emergency management systems and capabilities.

2 Data and related definition

2.1 Data

Here we use daily precipitation data from 86 national basic meteorological stations in Guangdong from 1995 to 2020. The rainstorm and flood disasters data are sourced from the "Guangdong Province Disaster Prevention and Mitigation Yearbook" (Volume 1995-2020) and aligns with the "Statistics of Nature Disasters (Part 1): Basic Indicators" (GB/T 24438.1-2009). The data includes various disaster types, such as the number of affected population (referred to as Ap), affected crop areas (referred to as Ac), direct economic losses (referred to as L), the number of deceased individuals (referred to as Nd), and the number of collapsed buildings (referred to as Ncb).

Sea surface temperature (SST) data were obtained from the HadISST1 data (Rayner et al., 2003), featuring a temporal resolution of 1 month and a spatial resolution of 1°×1°. Geopotential height data were acquired from the NCEP-NCAR reanalysis 1 data (Kalnay et al., 1996), with a temporal resolution of 1 day and a spatial resolution of 2.5° × 2.5°.

In order to standardize the L across different years and mitigate the influence of economic variation, we have adjusted L to the equivalent values in 2020. Utilizing the GDP index provided in the "Guangdong Statistical Yearbook-2021", L were discounted based on the 2020 price level. The conversion formula is as follows:

Converted value of L in a certain year = Value of L in a certain year×(1+ the cumulative value of the GDP index in a certain year relative to 2020 over Guangdong Province)

Here, "the GDP index of Guangdong Province in a certain year relative to the cumulative value in 2020" represents the cumulative product of GDP index from the subsequent year to 2020 for Guangdong Province. For instance:

The converted value of L in 2015 = the value of L in 2015×(1+2016 GDP index×2017 GDP index×2018 GDP index×2019 GDP index×2020 GDP index)

https://doi.org/10.5194/egusphere-2024-957
Preprint. Discussion started: 15 April 2024

2.2 Related index definitions

2.2.1 Definition of DBW

DBW refers to the concentrated precipitation phenomenon surrounding the Dragon Boat Festival, observed both before and after the festival, which falls on the fifth day of the fifth lunar month. For practical purposes, the conventional DBW period is delineated as the time span form May 21 to June 20 (Hu et al., 2013; Sheng et al., 2023).

However, the "Dragon Boat Festival" in 2001, 2004, 2012 and 2020 did not fall within the above-mentioned time period, and catastrophic rainstorms still occurred on June 21-30 in 1995, 2004, 2010, 2012, 2020, 2021 and 2022. The daily average precipitation and the number of stations with daily precipitation ≥50 mm for 1995-2020 (Fig.1) also indicate significant peaks in daily precipitation and heavy rainstorm stations from June 21 to 26. In other words, the concentrated period of heavy precipitation has not concluded yet.

Therefore, this study redefines DBW as the 15 days before and after the "Dragon Boat Festival" in the lunar calendar, totalling 31 days. As shown in Fig. 1, the new DBW definition in this study not only captures the fundamental characteristics of traditional DBW but also encompasses more features of the continuous heavy precipitation process. This proves more conductive to decision-making services for disaster prevention and mitigation decision-making than the conventional definition. The correlation coefficient of the total precipitation of DBW between the operation and the new definition is 0.72 ($P<0.05$).

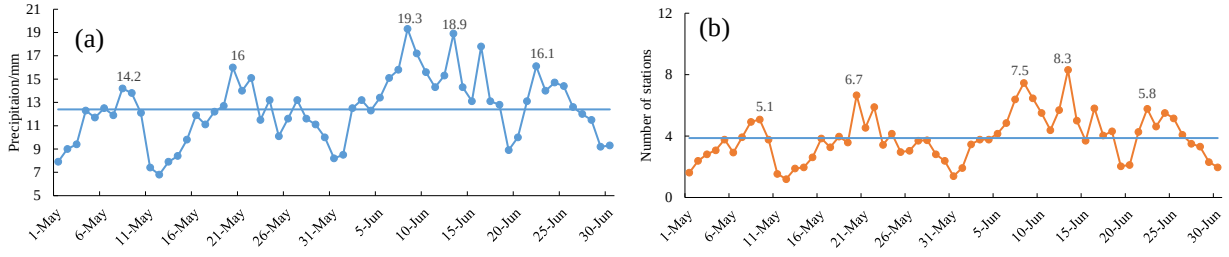

Figure 1. Average daily precipitation from 1995 to 2020 **(a, unit: mm)** and the number of stations with daily precipitation ≥50 mm from May 1st to June 30th **(b)**.

2.2.2 Precipitation comprehensive intensity index (*PCII*) during DBW

Based on the research on the evaluation of the rainstorm process in "the Comprehensive Intensity Evaluation Method of the Heavy Rain Process" (DB/T 2281-2021) and Hong (2020), the comprehensive intensity of precipitation in DBW is characterized using the total number of precipitation stations and precipitation intensity.

The total number of precipitation stations (referred to as *S*) is determined as the count of stations with daily precipitation ≥0.1 mm among the 86 stations during the DBW period in a specific year. The calculation formula is:

$$S = \sum_{t=1}^{D} S_t \,, \qquad (1)$$

https://doi.org/10.5194/egusphere-2024-957
Preprint. Discussion started: 15 April 2024

Where S is the total number of precipitation stations in one year, D is the number of precipitation days, S_t is the number of stations with precipitation ≥0.1 mm on the t-th day during the DBW period, and the same below.

The Precipitation Intensity (referred to as *PI*) is the average precipitation amount for S stations during the DBW period in a certain year. The calculation formula is:

$$PI = \frac{\sum_{t=1}^{D}\sum_{i=1}^{S_t} R_{t,i}}{S}, \quad (2)$$

Where *PI* represents the precipitation intensity index, and $R_{t,i}$ is the daily precipitation at the i-th station on the t-th day during the DBW period in a specific year

To ensure that the *PI* values are not too small, the *PI* index is multiplied by the square root of *S*, and the result is the index to represent the precipitation comprehensive intensity, hereinafter referred to as *PCII*. The calculation formula is:

$$PCII = PI \cdot S^{0.5}, \quad (3)$$

Based on our updated definition, torrential precipitation (daily precipitation ≥50 mm) and heavy precipitation (50 mm> daily precipitation≥25 mm) collectively constituted 30% and 56% of the overall precipitation, respectively, exhibiting strong correlation coefficients of 0.97 and 0.99. Consequently, from the standpoint of assessing precipitation intensity, the total precipitation can effectively serve as representative measure for the intensity of heavier precipitation, including rainstorm and heavy rain.

2.2.3 Comprehensive disaster index (*CDI*) during DBW

The "Handbook for Operation Climate Techniques of Guangdong Province" (2008) delineates and categorizes the intensity of DBW disaster based on the number of precipitation days, a method deemed inadequate for capturing the actual disaster scenario. Therefore, drawing inspiration from the works of Yang et al. (2018), the concurrent consideration of five disaster indicators--Ap, Ac, L, Nd and Ncb--was adopted. Subsequently, these 5 indices were normalized to derive corresponding indices I_{Ap}, I_{Ac}, I_L, I_{Nd} and I_{Ncb}, respectively. To achieve normalization, each of the five index factors was assigned equal weights of 0.2. The comprehensive disaster index (*CDI*) during the DBW period in a given year in Guangdong province is then represented by the summation of these five normalized factors. The calculation is expressed as follows:

$$CDI = 0.2 \times (I_{Ap} + I_{Ac} + I_L + I_{Nd} + I_{Ncb}), \quad (4)$$

Where $I_{Ap} = \frac{Ap-\overline{Ap}}{\sigma_{Ap}}, I_{Ac} = \frac{Ac-\overline{Ac}}{\sigma_{Ac}}, I_L = \frac{L-\bar{L}}{\sigma_L}, I_{Nd} = \frac{Nd-\overline{Nd}}{\sigma_{Nd}}, I_{Ncb} = \frac{Ncb-\overline{Ncb}}{\sigma_{Ncb}}$, 0.2 is the weight of the five indicators, σ is the mean squared error of the corresponding sample, and the formula is as follows:

$$\sigma = \sqrt{\frac{1}{n}\sum_{j=1}^{n}(X_j - \bar{X})^2}, \quad (5)$$

Where X is the sample of the corresponding indicator, X_j is the j-th sample number, n is the total number of corresponding indicator's samples, and $\bar{X}$ is the average value of the corresponding indicator.

https://doi.org/10.5194/egusphere-2024-957
Preprint. Discussion started: 15 April 2024

3 Results analysis

3.1 Classification of *PCII* during DBW

Following the arrangement of 1995 to 2020 *PCII* values in ascending order, the percentile method (Hyndman and Fan, 1996) was employed for grade categorization. By establishing the thresholds at the *PCII* percentile corresponding to 50% and 80%, the intensity indexes are classified into three levels: normal, heavy and extreme heavy (refer to Table 1).

Table 1. Classification of *PCII* during DBW.

Classification	Normal	Heavy	Extreme Heavy
PCII	*PCII* ≤652.45	652.45< *PCII* ≤821	*PCII* >821

Judging from the *PCII* for the years 1995-2020 (Fig. 2), 5 years (2008, 2006, 2005, 2001, and 2018) fall into the extreme heavy level, collectively accounting for 19.2% of the total. Additionally, 8 years (2010, 2007, 1998, 2019, 2009, 2003, 2014 and 2012) are categorized as heavy level, constituting 30.8% of the total. The remaining 13 years are classified as normal level, making up 50% of the total. Notably, the *PCII* peak appeared in the first decade of the 21st century, particularly concentrated between 2005 and 2010. Following a downward trend in 2011-2015, the *PCII* experienced a rapid and pronounced second peak in 2016-2019.

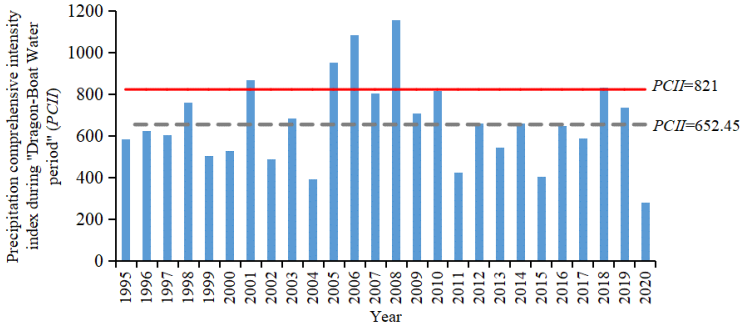

Figure 2. *PCII* during DBW from 1995 to 2020

https://doi.org/10.5194/egusphere-2024-957
Preprint. Discussion started: 15 April 2024

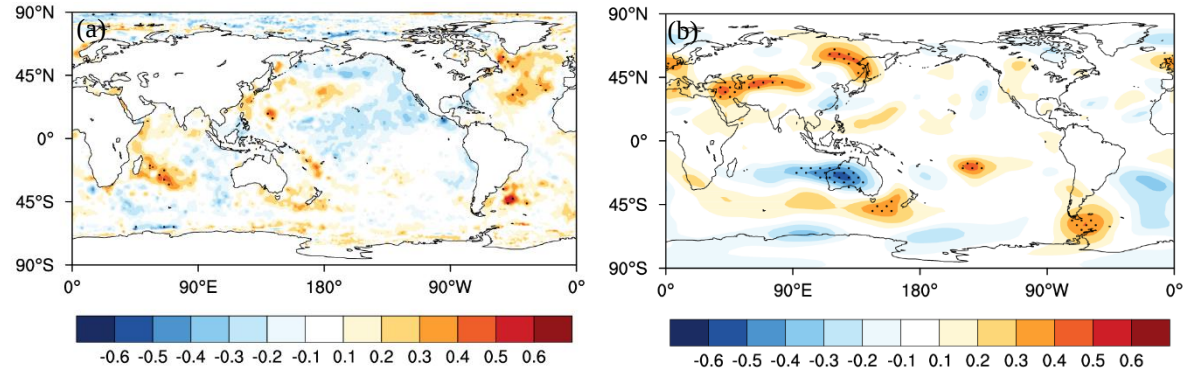

Figure 3. Correlation distributions between *PCII* and the SST field in May **(a)**, and the 500hPa geopotential height field in June **(b)**.

The correlation between *PCII* during DBW and precipitation in June is notably high, reaching 0.82. Consequently, utilizing June circulation is deemed reasonable for characterizing its impact on DBW. Specifically, during May, when Central Pacific (CP) experiences colder Sea Surface Temperature anomalies (SSTA), while the eastern region of the Philippines and the Atlantic register warmer conditions along with a positive phase of the India Ocean Dipole (IOD) (Fig. 3), *PCII* tends to be more pronounced during the ensuing DBW period.

In the subsequent June, a low-pressure anomaly manifests over Guangdong, surrounded by three anomalous high pressures: the South Asian high, the Okhotsk high, and the South China Sea (SCS) and western Pacific subtropical high (SCSSH). Anomalies in geopotential height near 120°E reflect the influence of the East Asia/Pacific (EAP) teleconnection. The correlation coefficients between *PCII* and the subtropical high ridge location index in SCS and the EAP index are -0.50 and -0.37, respectively, both statistically significant at the 95% confidence level (Fig.4). Favorable SST pattern conductive to heavy precipitation in DBW involve meridional SSTA in the western Pacific and zonal SSTA with a positive IOD phase. These conditions are conducive to tropical convective anomalies link to the EAP teleconnection, as highlighted in previous studies (Huang, 2004; Chen and Zhai, 2015). Furthermore, the variation in the EAP is related to the variability in the SCSSH. The configuration of the southward SCSSH, the northward South Asian high, and Okhotsk high, along with the EAP phase, has been reported by Zhao et al. (2020) to be responsible for persistent heavy precipitation over SC, creating a narrow quasi-stationary meridional positive isentropic potential vorticity channel on the inclined 345 K isentropic surface, facilitating the interaction between cold and warm-wet air.

https://doi.org/10.5194/egusphere-2024-957
Preprint. Discussion started: 15 April 2024

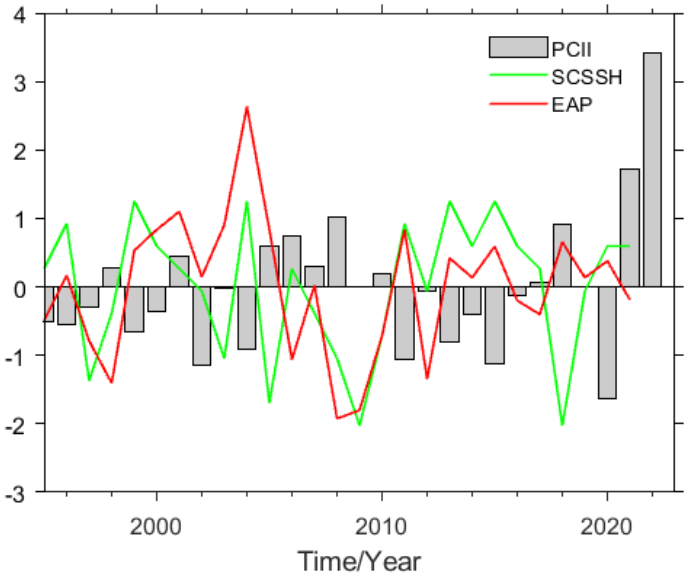

Figure 4. Time series of *PCII* (bar) and subtropical high ridge location index in South China Sea index (SCSSH; green line) and EAP index (red line) (Correlation coefficients between PCII and SCSSH, EAP are -0.50 and -0.37, respectively)

3.2 Classification of *CDI* during DBW

Table 2 presents information on disaster, *PCII* and *CDI* during the DBW period from 1995 to 2020. The table also includes Ap, Ac, L, Nd, Ncb. It is evident from the data that the most severe disaster occurred in 2005, marked by the highest instances of Ncb, Nd and L. Following closely is the 2008 disaster, characterized by a significant impact on the population and agricultural areas affected by disasters.

Table 2. Disaster information and *PCII* and *CDI* during DBW period from 1995 to 2020

Year	Ap (10,000 people)	Ac (10,000 hectares)	L (100 million CNY)	Nd (people)	Ncb (10,000 rooms)	*PCII*	*CDI*
2020	0	0	0	0	0	279.8	-0.624
2019	73.87	7.85	96.861	25	0.521	733.4	0.319
2018	0.39	0	0.355	0	0.001	830.6	-0.622
2017	14.694	0.39	3.381	0	0.01	586.5	-0.589
2016	27.71	1.669	6.346	2	0.029	645.8	-0.510
2015	0.139	0.043	0.552	0	0.002	401	-0.621
2014	141.11	8.195	118.696	18	1.981	660.9	0.607
2013	1.831	0.284	1.386	1	0.035	544.9	-0.593

https://doi.org/10.5194/egusphere-2024-957
Preprint. Discussion started: 15 April 2024

2012	61.85	4.685	33.645	13	0.199	659.1	-0.159
2011	23.16	1.54	9.155	1	0.016	424.7	-0.524
2010	176.345	12.31	65.053	8	1.203	814.6	0.315
2009	93.24	5.199	22.589	7	0.081	705.5	-0.246
2008	928	40.9	225.706	33	1.04	1154.3	2.471
2007	233	13.17	63.348	25	2.082	801.6	0.748
2006	104.28	9.805	89.366	21	0.804	1083.3	0.364
2005	485.48	24.09	248.873	70	5.853	952.8	2.991
2004	0	0	0.486	0	0	390.1	-0.623
2003	16.88	0.453	3.545	7	0.075	682.5	-0.484
2002	0	0	0	0	0	486.2	-0.624
2001	200.93	10.35	62.084	19	0.93	868.5	0.386
2000	0	0	0	0	0	526.9	-0.624
1999	0	0	0	0	0	503.9	-0.624
1998	36	0.56	23.311	13	0.057	757.9	-0.328
1997	52.75	2.26	11.006	3	0.038	603.1	-0.444
1996	63.82	3.26	43.309	4	0.231	623.6	-0.270
1995	143.64	10.55	74.001	15	0.886	582	0.309

Similar to the *PCII* level classification method in Section 3.1, here we also used the percentile method (Hyndman and Fan, 1996) to classify the *CDI* during DBW period into three levels: low, medium and high (Table 3).

Table 3. Classification of *CDI* during DBW

Classification	Low	Medium	High
CDI	*CDI*≤-0.39	-0.39<*CDI*≤0.37	*CDI* >0.37

According to the *CDI* spanning from 1995 to 2020, the high-risk level was observed in 5 years: 2005, 2008, 2007, 2014, 2001, collectively constituting 19.2%, with 2005 being the highest. Medium-level risk was recorded in 8 years: 2006, 2019, 2010, 1995, 2012, 2009 and 1996, making up 30.8%. The remaining 13 years exhibited a low-risk grade, accounting for 50.0%.

https://doi.org/10.5194/egusphere-2024-957
Preprint. Discussion started: 15 April 2024

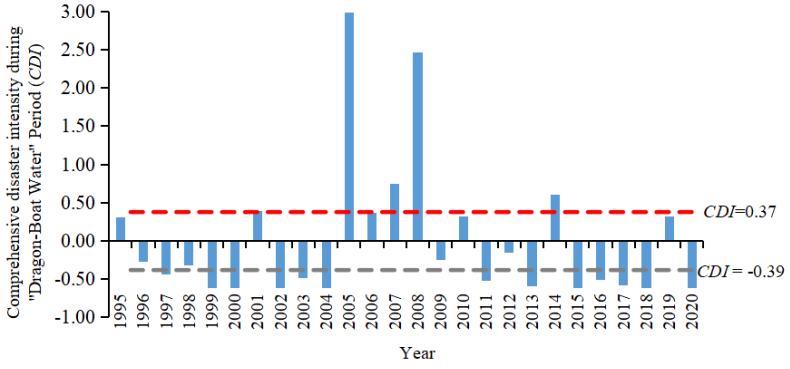

Figure 5. The interannual variation of *CDI* during DBW period from 1995 to 2020.

When comparing corresponding year between the *PCII* and *CDI* during DBW (Table 4), it is observed that 60% of the years with extreme heavy precipitation accounted for 60% of the years with severe disasters, namely high *CDI*. Additionally, 62.5% of the years with heavy precipitation contributed to 62.5% of the years with medium *CDI*, and 84.6% of the years with normal precipitation were associated with 84.6% of the years with low *CDI*. Consequently, there is a strong correspondence between *PCII* and *CDI*. While a majority of extreme heavy precipitation years coincide with high comprehensive disaster intensity, it is noteworthy that heavy or normal level precipitation can sometimes result in severe disasters, that is high comprehensive disaster intensity.

The research indicates that although precipitation serves as a primary factor causing flood disasters, the interplay of disaster-causing factors and the disaster-prone environment, along with the affected region, collectively determines the magnitude of the natural disaster. Additionally, the study highlights a concentration of heavily disaster-affected years during the period of intense DBW precipitation from 2005 to 2010, whereas the degree of disaster was relatively low in 2015-2020 (Fig.5). This outcome may be attribute to inter-annual variations in precipitation, advancement in forecasting technology, strengthened defence measures, and the reinforcement of disaster prevention and mitigation responses in the recent years.

Table 4. Corresponding years for different levels of *PCII* and *CDI* during DBW.

Indexes	Normal /Low	Heavy /Medium	Extreme heavy/High
PCII	2016, 1996, 1997, 2017, 1995, 2013, 2000, 1999, 2002, 2011, 2015, 2004, 2020	2010, 2007, 1998, 2019, 2009, 2003, 2014, 2012	2008, 2006, 2005, 2001, 2018
CDI	1997, 2003, 2016, 2011, 2017, 2013, 2015, 2018, 2004, 1999, 2000, 2002, 2020	2006, 2019, 2010, 1995, 2012, 2009, 1996, 1998	2005, 2008, 2007, 2014, 2001

Annotate: Within the same level, the different years between *PCII* and *CDI* are underlined.

https://doi.org/10.5194/egusphere-2024-957
Preprint. Discussion started: 15 April 2024

Normalized the five indicators: Ap, Ac, L, Nd and Ncb. The proportion of each disaster indicator is calculated annually (Fig. 6). The findings indicate that the Ap and Ac consistently emerge as the primary disaster factors, while Ncb consistently represents the smallest impact each year. Notably, during the period of heightened severe disasters from 2005 to 2010, Ap accounted for the largest proportion among the five disaster indicators, ranging from approximately 0.22 to 0.43.

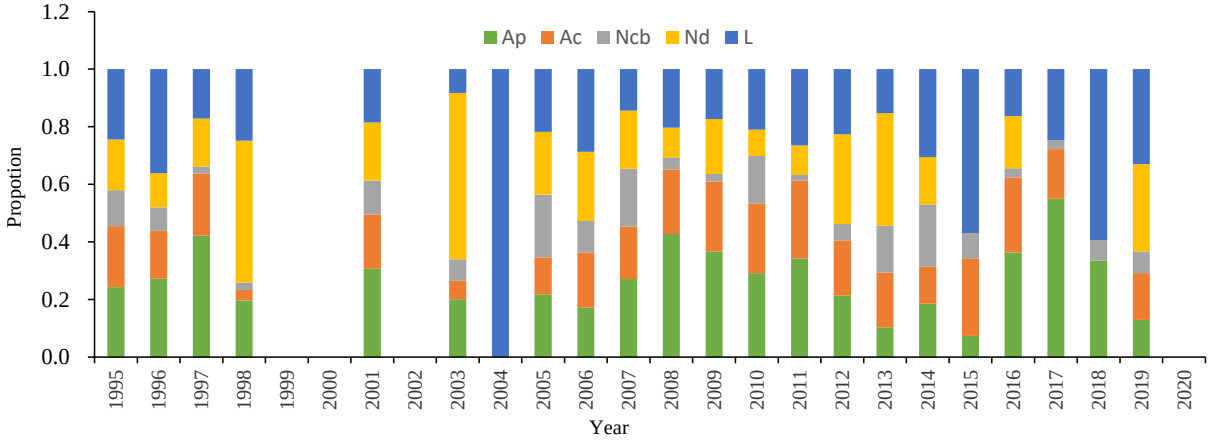

Figure 6. The proportion of the five disasters of DBW from 1995 to 2020.

3.3 The correlation between *PCII* and *CDI*

Upon fitting the *PCII* and *CDI* during DBW, a noticeable positive correlation emerges with a coefficient of 0.72 (at a significant level $p<0.05$) (Fig 7a). The correlations between Ap, Ac, L, Nd and Ncb with *PCII* are 0.70, 0.74, 0.49, 0.68 and 0.71, respectively, with the coefficient between *PCII* and Ac being the largest, followed by Ap and L. In the regression equations depicting the relationship between the 5 disaster indicators and *PCII* (Fig. 7b-f), the quadratic coefficient for Ap is the largest, measuring 0.0014. This observation suggests that, to a certain extent, an increase in the intensity of precipitation during DBW is associated with a higher likelihood of expanding the affected area of crops, impacting a larger number of affected population and incurring direct economic losses. Notably, the number of affected population by the disaster exhibits a particularly pronounced upward trend, aligning with the observation that the affected population constitutes the largest proportion among the different disaster types in the disaster-impacted years, as discussed in Section 3.2.

https://doi.org/10.5194/egusphere-2024-957
Preprint. Discussion started: 15 April 2024

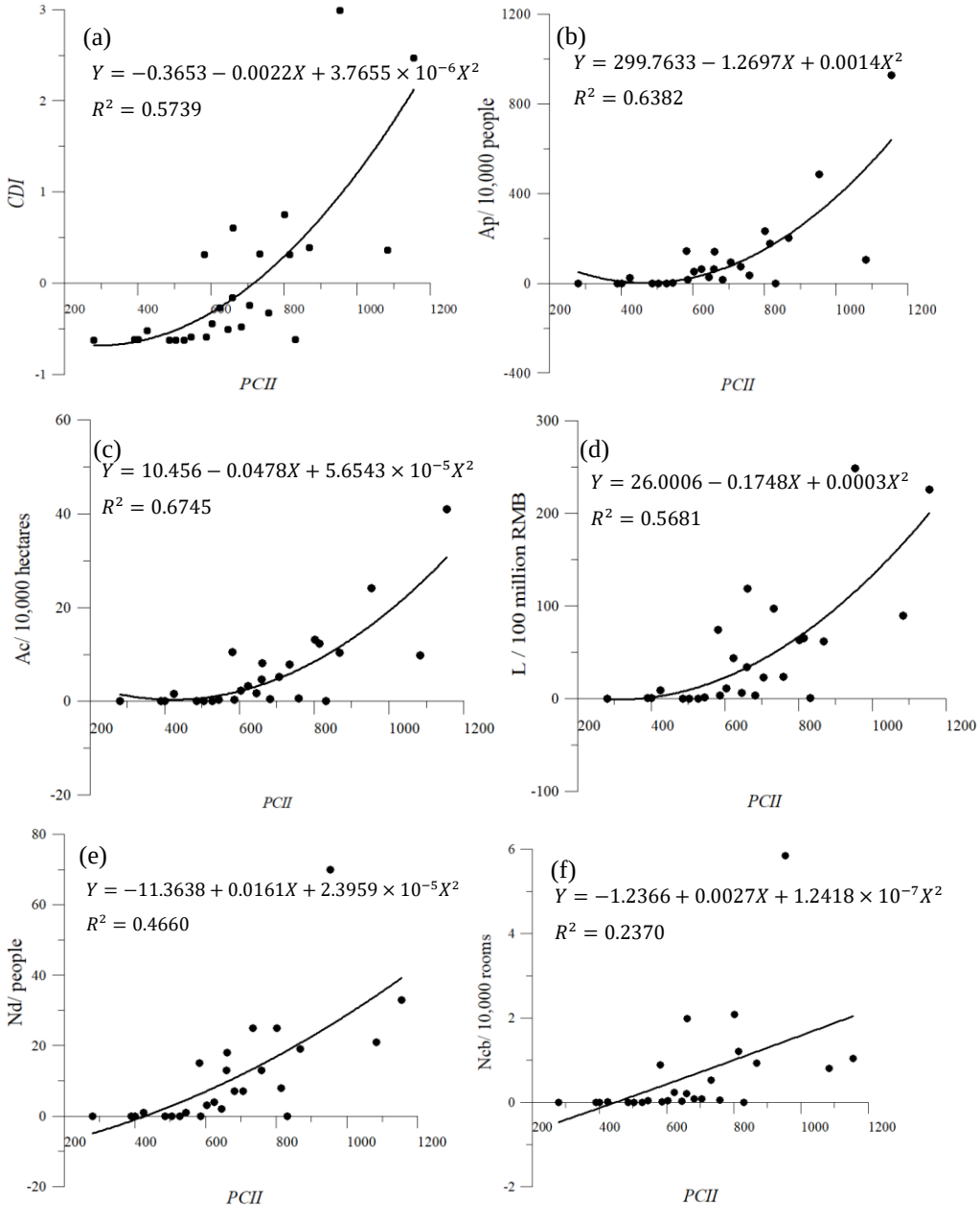

Figure 7. Relationships between *CDI* **(a)**、Ap **(b)**、Ac **(c)**、L **(d)**、Nd **(e)**、Ncd **(f)** and *PCII* during DBW period.

Over the past 26 years, on average (Table 5), during years characterized by extreme heavy precipitation intensity in the DBW period, the number of affected population averaged 3,438,200, while the affected area of crops covered 170,300 hectares. Moreover, the death toll averaged around 29, and approximately 17,300 houses collapsed. This scenario illustrates the

https://doi.org/10.5194/egusphere-2024-957
Preprint. Discussion started: 15 April 2024

significant impact of extreme precipitation on various disaster indicators. Furthermore, the direct economic loss, when converted to 2020 values, amounted to 12.528 billion CNY.

Transitioning to years with heavy precipitation intensity during DBW, the average number of affected population was 1,040,400, with the affected area of crops spanning 65,500 hectares. Additionally, the direct economic loss, when converted to 2020 values, was estimated at 5.338 billion CNY. About 15 people, on average, lost their lives, and around 7,700 houses collapsed. These findings underscore the substantial consequences associated with periods of elevated precipitation intensity. Moving on to the average years with normal precipitation intensity during DBW, the number of affected population averaged 252,100, with the affected area of crops covering 15,400 hectares. Furthermore, the direct economic loss, converted to 2020 values, stood at 1.151 billion CNY. On average, around 2 people lost their lives, and approximately 1,000 houses collapsed. It is crucial to note that specific disaster losses are influenced by various factors, including the natural environment, economic development, and defence measures, highlighting the complexity of disaster dynamics.

Table 5 Averaged disaster characteristics corresponding to the different *PCII* levels during DBW period.

Levels of *PCII*	Ap (10,000 people)	Ac (10,000 hectares)	L (100 million CNY)	Nd (people)	Ncb (10,000 rooms)
Extreme heavy	343.82	17.03	125.28	28.60	1.73
Heavy	104.04	6.55	53.38	14.5	0.77
Normal	25.21	1.54	11.51	2.00	0.10

In summary, the process of classifying and evaluating the risk level of DBW is illustrated in Fig.8.

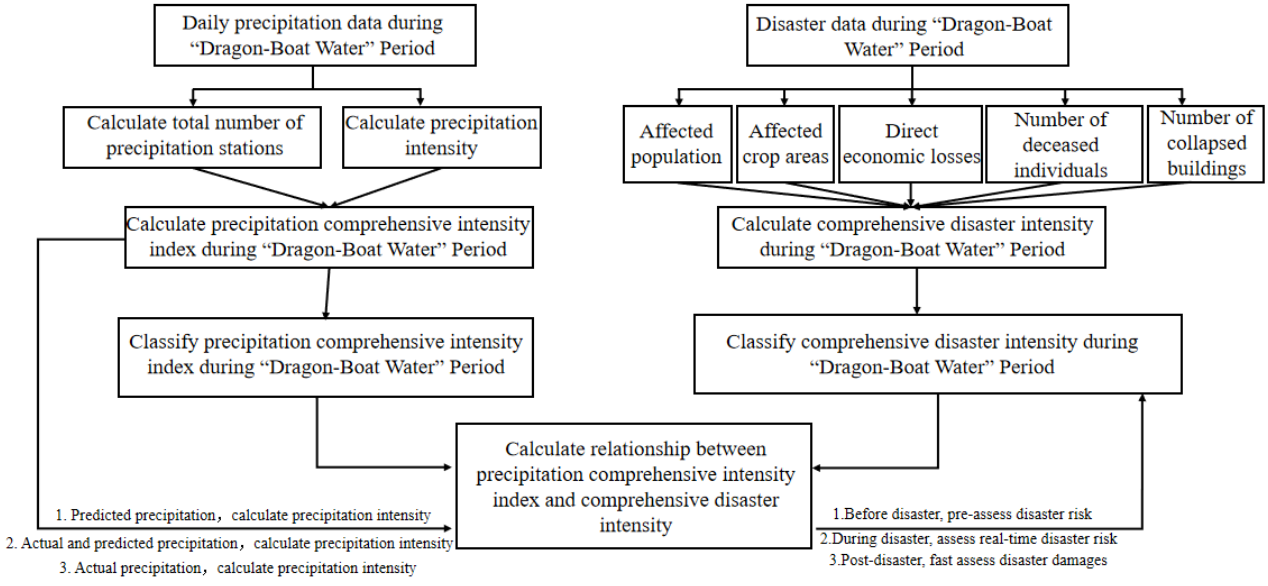

https://doi.org/10.5194/egusphere-2024-957
Preprint. Discussion started: 15 April 2024

Figure 8. Flow chart of risk level classification and disaster assessment during DBW period.

In conclusion, the comprehensive intensity level of DBW precipitation serves as a key indicator for understanding the corresponding comprehensive disaster grades. The connection between precipitation and disasters during the DBW period provides a basis for predicting the relevant comprehensive disaster level. In general, higher intensity and impact of natural disasters correlate with a large number of individuals and communities being exposed to these disasters, thereby increasing the potential for significant losses.

4 Conclusion

Drawing insights from the daily precipitation data from 86 national meteorological observation stations in Guangdong and flood disaster records spanning the years 1995 to 2020, the precipitation comprehensive intensity index (*PCII*) is defined by the combined influence of the total number of precipitation stations and precipitation intensity during the DBW period. Simultaneously, the comprehensive intensity index (*CDI*) is derived through the standardized equal-weighted impact assessment of affected population, affected crop areas, direct economic losses, the number of deceased individuals and collapsed buildings. This study delves into the relationship between the different levels of comprehensive intensity precipitation and their associated disaster risk grades over the DBW period in Guangdong province.

Over the 1995-2020 timeframe, 19.2% of *PCII* fell into the extreme heavy level, 30.8% in the heavy level, and 50.0% in the normal level. The most prominent peak in comprehensive precipitation intensity during DBW occurred in the first decade of the 21st century, primarily in 2005-2010, with the second strongest peak observed in 2016-2019, and the highest peak in 2008. Consistent with *PCII*, over the past 26 years, *CDI* also revealed 19.2% high-risk level, 30.8% medium level and 50.0% the low level, with the highest recorded in 2005, closely followed by 2008. The peak value of comprehensive disaster index aligns with the corresponding peaks in comprehensive precipitation intensity. Among the 5 types of disasters considered, direct economic losses and the number of the affected population account for the largest proportions. Notably, the primary disaster type in high-risk years is the number of affected population. In 2005, the highest-risk year in the past 26 years, the death toll and direct economic losses reached their maximum, while in 2008, the disaster-affected population and agricultural area peaked, marking it as the second-highest year in comprehensive disaster severity.

The *PCII* exhibits a positive correlation with the *CDI* and the 5 indicators representing different disaster types. A heavier comprehensive intensity of DBW precipitation corresponds to a higher comprehensive disaster index. The affected area of crops, the number of affected population, and the number of fatalities are positively correlated with the comprehensive disaster index.

5 Discussion

Currently, the civil affairs department's disaster data for 2021 and 2022 are still pending completion. However, based on the "Dragon Boat Water" precipitation data, the comprehensive precipitation intensity indexes are calculated to be 611 and 869.4

https://doi.org/10.5194/egusphere-2024-957
Preprint. Discussion started: 15 April 2024

for 2021 and 2022, respectively falling within the normal and extreme heavy grade of *PCII*. Utilizing a rapid post-disaster assessment formula, the resulting comprehensive disaster indexes are -0.3038 and 0.5682, indicating medium and high-risk levels, respectively. Notably, 2022 marks the 4th highest precipitation and 5th heaviest disaster level since 1995, aligning closely with the actual situation in 2022. This underscore the potential utility of the index for post-disaster assessment when complete disaster data is not yet available.

Looking ahead, the comprehensive intensity can be computed based on predicted precipitation during the DBW period. This allows for pre-disaster risk assessment, ongoing assessment during disasters, and rapid post-disaster assessment, serving as a valuable tool in safeguarding Guangdong's social and economic development.

It's important to acknowledge that this research primarily focuses on overall disaster risk level in Guangdong province during the DBW period. Future endeavours should pay more attention to further zoning and risk assessment based on data related to different vulnerable disaster types and precipitation in various cities and counties within Guangdong. Additionally, considering that the greater the vulnerability of the disaster-bearing body, the higher the potential losses, and future assessments should incorporate the vulnerability of the disaster-bearing body itself as factor. This holistic approach aims to enhance local meteorological services, emphasizing the need to improve forecast accuracy and, based on forecast results, swiftly execute disaster reduction and rescue arrangement. This proactive approach ensures the sustainable and healthy development of the economy, leveraging meteorological functions to drive prosperity and mitigate potential disasters.

Financial support. This study was funded by the National Natural Science Foundation of China (U2142205 and 42075173); Guangdong Major Project of Basic and Applied Basic Research (2020B0301030004); Special Fund of China Meteorological Administration for Innovation and Development (CXFZ2023J027); and Special Fund for Forecasters of China Meteorological Administration (CMAYBY2020-094).

Data availability. The daily precipitation data are available at China Meteorological Data Network (http://data.cma.cn). The SST data are available at https://www.cen.uni-hamburg.de/en/icdc/data/ocean/hadisst1.html. Geopotential height data from NCEP-NCAR are available at https://psl.noaa.gov/data/gridded/data.ncep.reanalysis.html.

Author contributions. Yamin Hu conceived the research framework and developed the methods, wrote the first draft and provided funding. Jiang Xiaocen is responsible for code compilation, data analysis, graphic visualization and first draft writing. Wang Juanhuai participated in the data collection and data arrangement of this study. Zhao Liang designed the method and revised the first draft. Huang Guanrong participated in preparing the data and performing analysis. All authors discussed the results and contributed to the final version of the paper.

Competing interest. The authors declare that they have no conflict of interest.

https://doi.org/10.5194/egusphere-2024-957
Preprint. Discussion started: 15 April 2024

References

Bouttier, F. and Marchal, H.: Probabilistic short-range forecasts of high precipitation events: optimal decision thresholds and predictability limits, EGUsphere [preprint], https://doi.org/10.5194/egusphere-2023-3111, 2024.

Cheng, J., Zhao, Y., Zhi, R., and Feng, G.: Meridional circulation dominates the record-breaking "Dragon Boat Water" precipitation over south China in 2022, Front. Earth Sci., 10, 1032313, https://doi.org/10.3389/feart.2022.1032313, 2023.

Ding, Y. H., and Chan, J. C. L.: The East Asian summer monsoon: an overview, Meteorol. Atmos. Phys., 89, 117–142, https://doi.org/10.1007/s00703-005-0125-z, 2005.

Editorial Committee: Handbook for operation climate techniques of Guangdong province, China Meteorological Press, Beijing, China, ISBN 9787502944995, 2008.

Han, X., Sun, X., Li, S., Wang, M., Li, G., Chen, Y., Wang, G.: Disaster-causing index of rainstorm and pre-assessment of disaster effect in Liaoning province, J Meteor Environ 30, 80-84, 2014.

Hong, G.: Localized revision and application of assessing indices for regional heavy precipitation events in Hubei Province, Torrential Rain and Disasters, 39, 470-476, 2020.

Hu, H., Xuan, C., Zhu, L.: The pre-event risk assessment of Beijing Urban Flood, J Appl Meteor Sci, 24, 99-108, 2013.

Hu, Y., Du, Y., Luo, X.: Precipitation patterns during the "Dragon Boat Water" in South China for the recent 49 years, Meteorol Mon, 39, 1031-1041, https://doi.org/10.7519/j.issn.1000-0526.2013.08.010, 2013.

Hu, Y., Si, D., Liu, Y., Zhao, L.: Investigations on moisture transports, budgets and sources responsible for the decadal variability of precipitation in southern China, J Trop Meteor, 22, 402-412, https://doi.org/10.16555/j.1006-8775.2016.03.014,2016.

Huang, G.: An index measuring the interannual variation of the East Asian summer monsoon—The EAP index, Adv. Atmos. Sci., 21, 41–52, https://doi.org/10.1007/BF02915679, 2004.

Huang, Z., Liu, W., Zhang, Y., Liang, M., Liu, Y.: Design of weather-based claiming index for early rice "Dragon Boat Rain" disaster insurance, Torrential Rain and Disasters, 38, 676-682, 2019.

Hyndman, R. J. and Fan, Y. N.: Sample Quantiles in Statistical Packages, The American Statistician, 50, 361–365, https://doi.org/10.1080/00031305.1996.10473566, 1996.

Kalnay, E., Kanamitsu, M., Kistler, R., Collins, W., Deaven, D., Gandin, L., Iredell, M., Saha, S., White, G., Woollen, J., Zhu, Y., Chelliah, M., Ebisuzaki, W., Higgins, W., Janowiak, J., Mo, K. C., Ropelewski, C., Wang, J., Leetmaa, A., Reynolds, R., Jenne, R., and Joseph, D.: The NCEP/NCAR 40-year reanalysis project, Bulletin of the American Meteorological Society, 77, 437–472, https://doi.org/10.1175/1520-0477(1996)077<0437:TNYRP>2.0.CO;2, 1996.

Lin, L., Wu, N., Huang, Z., Cai, A.: Causality analysis of infrequent dragon-boat precipitation in Guangdong province in 2008, Meteorol Mon, 35, 43–50, https://doi.org/10.7519/j.issn.1000-0526.2020.11.003, 2009.

https://doi.org/10.5194/egusphere-2024-957
Preprint. Discussion started: 15 April 2024

Liu, B., Zhu, C., Xu, K., Ma, S., Lu, M., Han, X., and Hua, L.: Record-breaking pre-flood precipitation over South China in 2022: role of historic warming over the Northeast Pacific and Maritime Continent, Clim Dyn, 61, 3147–3163, https://doi.org/10.1007/s00382-023-06734-6, 2023.

Luo, Y., Wu, M., Ren, F., Li, J., and Wong, W. K.: Synoptic situations of extreme hourly precipitation over China, J. Climate, 29, 8703–8719, https://doi.org/10.1175/JCLI-D-16-0057.1, 2016.

Luo, Y., Xia, R., and Chan, J. C. L.: Characteristics, physical mechanisms, and prediction of pre-summer rainfall over South China: research progress during 2008–2019, Journal of the Meteorological Society of Japan, 98, 19–42, https://doi.org/10.2151/jmsj.2020-002, 2020.

Peng, J., Wei, H., Wu, W., Liu, Y., Wang, Y.: Storm flood disaster risk assessment in urban area based in the simulation of land use scenarios: A case of Maozhou Watershed in Shenzhen City. Acta Ecologica Sinica, 38, 3741-3755, 2018.

Qian, W., Ai, Y., Chen, L., Li H.: Anomalous synoptic pattern of typical dragon boat precipitation process in Guangdong province, J Trop Meteorol, 36, 433–443, https://doi.org/10.16032/j.issn.1004-4965.2020.040, 2020.

Quan, R. S.: Rainstorm waterlogging risk assessment in central urban area of Shanghai based on multiple scenario simulation, Nat Hazards, 73, 1569–1585, https://doi.org/10.1007/s11069-014-1156-x, 2014.

Rayner, N. A., Parker, D. E., Horton, E. B., Folland, C. K., Alexander, L. V., Rowell, D. P., Kent, E. C., and Kaplan, A.: Global analyses of sea surface temperature, sea ice, and night marine air temperature since the late nineteenth century, J. Geophys. Res., 108, 2002JD002670, https://doi.org/10.1029/2002JD002670, 2003.

Sheng, B., Wang, H., Li, H., Wu, K., and Li, Q.: Thermodynamic and dynamic effects of anomalous dragon boat water over South China in 2022, Weather and Climate Extremes, 40, 100560, https://doi.org/10.1016/j.wace.2023.100560, 2023.

Song, N., Ma, Z., Fan, G., Guo, H., Xu, Y.: A study of thresholds of rainstorm-flood hazard based on HBV-D hydrological model over the Jiangling River Basin, Journal of Southwest University (Natural Science Edition), 40(2), 186-192, https://doi.org/10.13718/j.cnki.xdzk.2018.02.026, 2018.

Wang, Y., Zhai, J., Gao, G., Liu, Q., and Song, L.: Risk assessment of rainstorm disasters in the Guangdong–Hong Kong–Macao greater bay area of China during 1990–2018, Geomatics, Natural Hazards and Risk, 13, 267–288, https://doi.org/10.1080/19475705.2021.2023224, 2022.

Wu, N., Lin, L., Zeng, Q., Wu, Z., Jin, R., Deng, W.: Causal analysis of consecutive torrential rains in Guangdong province before the onset of South China sea monsoon, J Appl Meteor Sci, 24, 129-139, 2013.

Wu, Y. N., Zhong, P. A., Zhang, Y., Xu, B., Ma, B., and Yan, K.: Integrated flood risk assessment and zonation method: a case study in Huaihe River basin, China, Nat Hazards, 78, 635–651, https://doi.org/10.1007/s11069-015-1737-3, 2015.

Wu, Z., Shen, Y., Wang, H., and Wu, M.: Assessing urban flood disaster risk using Bayesian network model and GIS applications, Geomatics, Natural Hazards and Risk, 10, 2163–2184, https://doi.org/10.1080/19475705.2019.1685010, 2019.

Xie, J., Hsu, P.-C., Hu, Y., Lin, Q., and Ye, M.: Disastrous persistent extreme rainfall events of the 2022 pre-flood Season in South China: causes and subseasonal predictions, J Meteorol Res, 37, 469–485, https://doi.org/10.1007/s13351-023-3014-9, 2023.

https://doi.org/10.5194/egusphere-2024-957
Preprint. Discussion started: 15 April 2024

Xie, Y., Han, S., You, L., Wang, Y., Yan, C.: Risk analysis of urban precipitation waterlogging in Tianjin City, Scientia Meteor Sinica, 24, 342-349, 2004.

Yang, C., Pan, A., Li, J., Wang, Y.: Grade division of meteorological disaster sensitive units based on emergency integrated management, Journal of Catastrophology, 33, 27-31, 2018.

Zhao, L., Liu, H., Hu, Y., Cheng, H., and Xiao, Z.: Extratropical extended-range precursors near the tropopause preceding persistent strong precipitation in South China: a climatology, Clim Dyn, 55, 3133–3150, https://doi.org/10.1007/s00382-020-05437-6, 2020.

Zheng, Y., Xue, M., Li, B., Chen, J., and Tao, Z.: Spatial characteristics of extreme rainfall over China with hourly through 24-hour accumulation periods based on national-level hourly rain gauge data, Adv. Atmos. Sci., 33, 1218–1232, https://doi.org/10.1007/s00376-016-6128-5, 2016.

Zhou, Y., Peng, T., Shi, R.: Research progress on risk assessment of heavy precipitation and flood disasters in China, Torrential Rain Disaster, 38, 494-501, 2019.